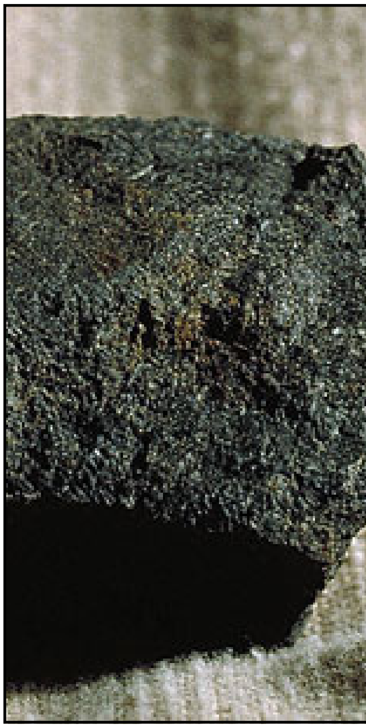

# Class 6

Physical Properties of Coal

1

## Particle Energy Equation

$$m_p C_p \frac{dT_p}{dt} = q_{conv} + q_{rxn} + q_{rad}$$

- $m_p = \rho_p V_p = \rho_p \frac{4}{3} \pi r_p^3$
- $q_{conv} = \theta h A_p \left(T_g - T_p\right)$
- $q_{rxn} = \dot{r}''_{rxn,p} A_p \Delta H_{rxn}$
- $q_{rad} = \epsilon_p \sigma A_p \left(T_\infty^4 - T_p^4\right)$
- $A_p = 4 \pi r_p^2$

2

## Particle Energy Equation

$$m_p C_p \frac{dT_p}{dt} = q_{conv} + q_{rxn} + q_{rad}$$

- $m_p = \rho_p V_p = \rho_p \frac{4}{3}\pi r_p^3$
- $q_{conv} = \theta h A_p (T_g - T_p)$
- $q_{rxn} = \Sigma \dot{r}''_{rxn,i} A_p \Delta H_{rxn,i}$
- $q_{rad} = \epsilon_p \sigma A_p (T_\infty^4 - T_p^4)$
- $A_p = 4\pi r_p^2$
- $Nu = \frac{h d_p}{k_g} = 2 + f(Re_p, Pr)$

3

**Reading Assignment:**

a. **Lee Smith Book, 154-168**
b. **Article by Merrick (*Fuel*, 62, 540-546, 1983)**
c. **Richards, A., D. Haycock, J. Frandsen, and T. H. Fletcher, "A Review of Coal Heating Value Correlations with Application to Coal Char, Tar, and Other Fuels," Fuel, 118942:1-16 (2021). DOI: 10.1016/j.fuel.2020.118942**

1. Discuss Figure 4.50 in the Lee Smith book.
2. What is meant by porosity, true density, apparent density, and internal surface area? Why are these quantities important in coal combustion? How do they vary as a function of coal rank? How do the these properties vary between chars and coals?
3. Please use your group to find and discuss the model proposed by Merrick for heat capacity.
4. Please compute the heat capacity in J/kg/K of the dried Argonne Premium Wyodak coal at temperatures from 300 K to 700 K.
5. Please compute the number distribution (# vs. diameter in microns) for the following mass distribution:

| Mesh Size (passing) | 400 | 325 | 270 | 250 | 200 | 170 | 150 |
|---|---|---|---|---|---|---|---|
| Weight (%) | 5 | 10 | 20 | 30 | 20 | 10 | 5 |

6. Search the web for the DuLong formula, which is used to compute the heating value of coal from the elemental composition. Calculate the heating value of the Illinois #6 Argonne Premium coal and compare the calculated value with the measured value.
7. Recalculate the heating value in problem #7 using the Mott-Spooner re-fit correlation in the paper by Richards et al. (2021).

4

# Figure 4.50

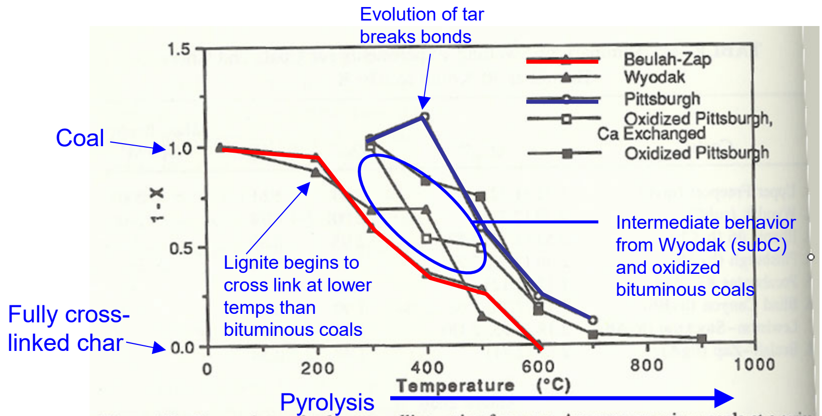


**Figure 50.** Comparison of solvent-swelling ratios for some Argonne premium coals at a series of pyrolysis final temperatures. Effects of oxidation and minerals on cross-linking behavior are shown for the Pittsburgh coal. The Beulah–Zap and Wyodak coals were pyrolyzed with a heating rate of 30 K/min while the Pittsburgh coal sample were pyrolyzed with a heating rate of 0.5 K/s (Solomon *et al.*, 1990).

5

# Particle Densities

1. True Density (He pyncnometry) $\dfrac{mass\ of\ solid}{volume\ of\ solid}$

2. Apparent Density

$$\frac{mass\ of\ solid}{volume\ of\ solid + volume\ of\ voids\ in\ solid}$$

3. Bulk Density

$$\frac{mass\ of\ solid}{volume\ of\ bed}$$

$V_{bed} = V_{solid} + V_{voids\ in\ solid} + V_{voids\ between\ particles}$

6

# True Particle Densities

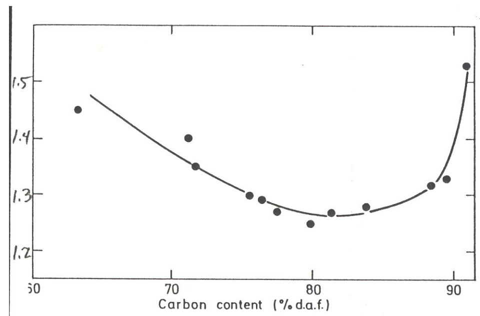


ıre 2 Variation of helium density of coals with carbon content

From Gan et al. Fuel, Vol. 51 (1972)

7

# Apparent Densities

- Hg porosimetry
  - Measure change in Hg volume as pressure increases
  - Interpret volume change
- Tap density
  - Weigh particles
  - Place in graduated cylinder
  - Tap to settle particles
  - Assume packing factor
  - Ratio of bulk densities ($\rho_b / \rho_{b,0}$) equals ratio of apparent densities ($\rho_a / \rho_{a,0}$)

8

MICROMERITICS AUTO-PORE 9200 V2.03 PAGE 2

New Mexico Blue Subbituminous

T.FLETCHER LP 11:19:50 5/18/88
REQ88423 COAL T103 PSOC 1445 HIGH TEMP HP 15:6:54 5/18/88
PNTR NUMBER +882 1250 K, 70 mm

Interparticle

Intraparticle

| PRESSURE PSIA | PORE DIAMETER MICRO-M | INTRUSION VOLUME CC/G | PORE SURFACE SQ-M/G | MEAN DIAMETER MICRO-M | DV |
|---|---|---|---|---|---|
| +1.4 | +129.6650 | +0.0000 | +0.0000 | +129.6650 | +0.0000 |
| +1.7 | +107.5830 | +0.0139 | +0.0005 | +118.6240 | +0.0139 |
| +2.0 | +90.9093 | +0.0510 | +0.0020 | +99.2459 | +0.0371 |
| +2.7 | +67.4971 | +0.1205 | +0.0055 | +79.2031 | +0.0695 |
| +4.0 | +45.4547 | +0.6439 | +0.0425 | +56.4758 | +0.5234 |
| +5.3 | +34.3604 | +1.2739 | +0.1057 | +39.9075 | +0.6300 |
| +7.9 | +22.7483 | +1.5055 | +0.1381 | +28.5543 | +0.2316 |
| +9.6 | +18.8785 | +1.5426 | +0.1453 | +20.8134 | +0.0371 |
| +11.9 | +15.1051 | +1.5704 | +0.1518 | +16.9918 | +0.0278 |
| +12.8 | +14.0699 | +1.5843 | +0.1556 | +14.5875 | +0.0139 |
| +13.9 | +12.9734 | +1.5936 | +0.1584 | +13.5216 | +0.0093 |
| +16.4 | +11.0279 | +1.6029 | +0.1615 | +12.0006 | +0.0093 |
| +20.8 | +8.6932 | +1.6215 | +0.1690 | +9.8605 | +0.0186 |
| +23.9 | +7.5433 | +1.6354 | +0.1759 | +8.1182 | +0.0139 |
| +25.7 | +7.0333 | +1.6354 | +0.1759 | +7.2883 | +0.0000 |
| +28.9 | +6.2484 | +1.6355 | +0.1759 | +6.6409 | +0.0000 |
| +33.5 | +5.3881 | +1.6402 | +0.1791 | +5.8183 | +0.0047 |
| +40.1 | +4.5020 | +1.6402 | +0.1792 | +4.9450 | +0.0001 |
| +45.6 | +3.9596 | +1.6450 | +0.1836 | +4.2308 | +0.0047 |
| +51.6 | +3.4946 | +1.6682 | +0.2086 | +3.7271 | +0.0232 |
| +60.8 | +2.9693 | +1.7007 | +0.2489 | +3.2320 | +0.0325 |
| +76.7 | +2.3527 | +1.7612 | +0.3397 | +2.6610 | +0.0604 |
| +93.9 | +1.9222 | +1.8124 | +0.4355 | +2.1375 | +0.0512 |
| +118.2 | +1.5264 | +1.8868 | +0.6082 | +1.7243 | +0.0744 |
| +140.6 | +1.2834 | +1.9334 | +0.7409 | +1.4049 | +0.0466 |
| +183.0 | +0.9863 | +2.0081 | +1.0040 | +1.1349 | +0.0747 |
| +232.6 | +0.7760 | +2.0782 | +1.3222 | +0.8812 | +0.0701 |
| +267.7 | +0.6742 | +2.1064 | +1.4779 | +0.7251 | +0.0282 |
| +334.2 | +0.5400 | +2.1627 | +1.8492 | +0.6071 | +0.0564 |
| +429.0 | +0.4207 | +2.2147 | +2.2823 | +0.4804 | +0.0520 |
| +530.5 | +0.3402 | +2.2621 | +2.7805 | +0.3805 | +0.0474 |
| +637.9 | +0.2829 | +2.2956 | +3.2104 | +0.3116 | +0.0335 |
| +800.1 | +0.2256 | +2.3295 | +3.7440 | +0.2543 | +0.0339 |
| +988.6 | +0.1826 | +2.3635 | +4.4105 | +0.2041 | +0.0340 |
| +1214.2 | +0.1486 | +2.3930 | +5.1229 | +0.1656 | +0.0295 |
| +1516.0 | +0.1191 | +2.4228 | +6.0134 | +0.1339 | +0.0298 |
| +1903.8 | +0.0948 | +2.4436 | +6.7893 | +0.1069 | +0.0207 |
| +2354.1 | +0.0767 | +2.4689 | +7.9706 | +0.0857 | +0.0253 |
| +2908.0 | +0.0621 | +2.4850 | +8.8989 | +0.0694 | +0.0161 |
| +3603.0 | +0.0501 | +2.5057 | +10.3792 | +0.0561 | +0.0208 |
| +4562.9 | +0.0396 | +2.5220 | +11.8322 | +0.0448 | +0.0163 |
| +5576.2 | +0.0324 | +2.5378 | +13.5914 | +0.0360 | +0.0158 |
| +6857.8 | +0.0263 | +2.5536 | +15.7365 | +0.0293 | +0.0157 |
| +8646.0 | +0.0209 | +2.5693 | +18.4062 | +0.0236 | +0.0157 |
| +10613.1 | +0.0170 | +2.5847 | +21.6436 | +0.0189 | +0.0153 |
| +13176.2 | +0.0137 | +2.5998 | +25.6000 | +0.0154 | +0.0152 |
| +16484.5 | +0.0109 | +2.6148 | +30.4615 | +0.0123 | +0.0150 |
| +20493.1 | +0.0088 | +2.6342 | +38.2900 | +0.0099 | +0.0193 |

9

from Sandia Report SAND88-8240, Coal Combustion Science
Quarterly Progress Report, January – March, 1988

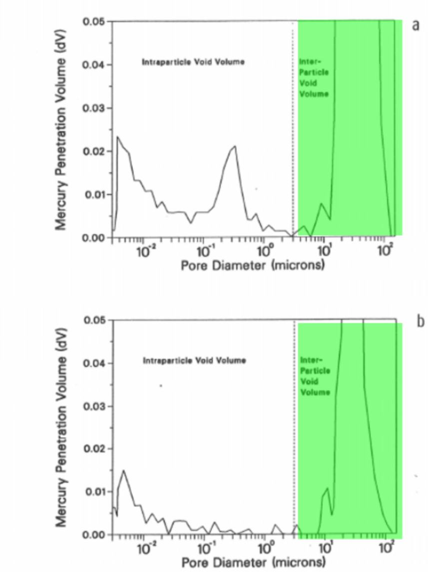


Figure 2. Incremental penetration volume from mercury porosimetry analysis of (a) Spherocarb particles (125 - 149 µm), and (b) PSOC 1415d Pittsburgh #8 high volatile bituminous coal particles (106-125 µm size fraction).

10

# Apparent Particle Densities

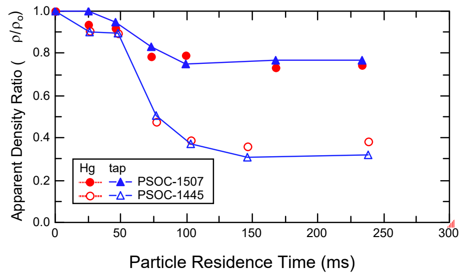


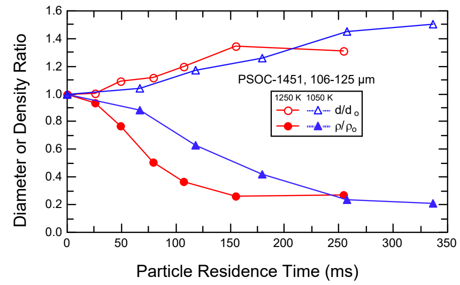


From Fletcher Sandia Milestone Report

11

## Heat Capacity of Coal

$$h = \int_{T_{ref}}^{T} C_p \, dT$$

$C_p$ (particle) = $x_{moist}\, C_{p,\,moist} + x_{org}\, C_{p,\,org} + x_{ash}\, C_{p,\,ash}$

Note: $C_p$ is a function of $T_{particle}$

Einstein's Formulation for $C_p$ (from Merrick, 1983):

**A. Simple**

$$C_p = (3R/a)\; g_1\{1200/T\} J/kg/K$$

$$a = \left[\sum y_n/\mu_n\right]^{-1}$$

where a = mean coal atomic weight, $y_n$ = mass fraction of element n, and μ = atomic weight of element n

$g_1$ is a function:

$$g_1\{z\} = \frac{\exp(z)}{[(\exp(z)-1)/z]^2}$$

R = universal gas constant (8314.3 N-m/K/kg-mol

**B. 2-stage (along bedding plane and perpendicular to bedding plane)**

$$C_p = (R/a)\; g_1\{380/T\} + 2g_1\{1800/T\}\; J/kg/K$$

Also note that enthalpy is calculated by Merrick as:

$$h = 3600(R/a)\; g_0\{1200/T\}\; J/kg \quad \text{or}$$
$$h = (R/a)\;[380 g_0\{380/T\} + 3600 g_0\{1800/T\}]\; J/kg$$

Where $g_0\{z\} = \dfrac{1}{\exp(z)-1}$

**C. $C_p$ for Ash**

$C_{p,\,ash}$ = 754 + 0.586 T (J/kg/K where T is in °C) or
$C_{p,\,ash}$ = 593 + 0.586 T (J/kg/K where T is in K)

12

Merrick Heat Capacities

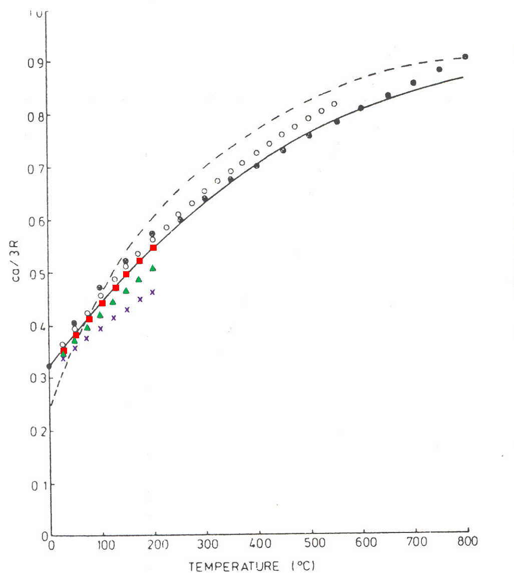


*Figure 2* Variation of *ca*/3*R* with temperature. ---, Simple Einstein model; ———, Einstein model with two characteristic temperatures. ●, Graphite; ○, coke; □, 35 wt% VM; △, 25 wt% VM; ×, 15 wt% VM



# Computed Heat Capacities

(Wyodak Coal)

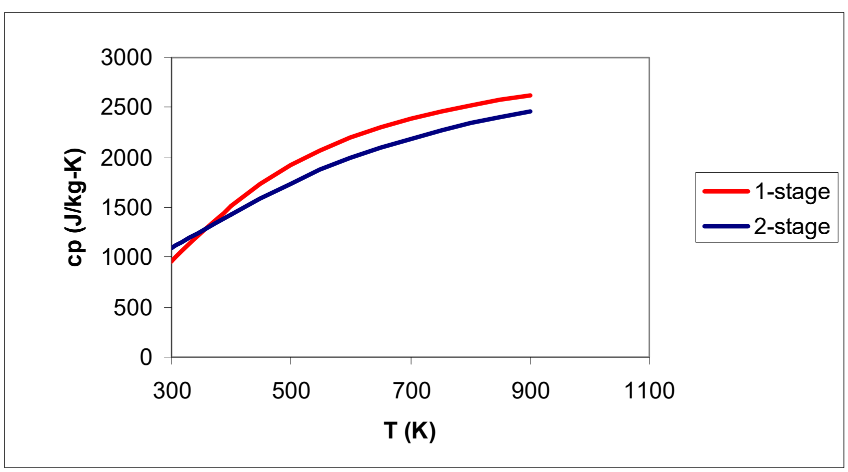

# Heat Capacities (Conclusions)

**Cautions about the Merrick model:**

- **Good for graphite and char (coke)**
- **Coal heat capacity data are limited**
- **Model does not fit data from different coal ranks very well!**
- **Coal data only extends to 200°C (573 K)**

**In other words, keep a look out for better heat capacity data!**

15

# Thermal Conductivities

- Atkinson and Merrick (1983) report that the thermal conductivities *k* of coal, semi-cokes and cokes (W m-1 K-1) can be correlated as follows:

  $k = (\rho_t/4511)^{3.5}\ T^{0.5}$

  where $\rho_t$ is the true density of the material (2260 kg $m^3$ for amorphous carbon, 1279 kg $m^3$ for coal)
- The temperature dependence of this correlation does not agree well with the findings of Badzioch, et al. (1964), which are approximately correlated by the following expression:

  $k = 0.23$ $\quad$ $300\ K < T < 773\ K$

  $k = (T/255) – 2.8$ $\quad$ $773\ K < T < 1173\ K$
- The two expressions agree at temperatures below 800 K, but the data and correlation from Badzioch and coworkers indicate significantly higher thermal conductivities at temperatures greater than 800 K.

Recommendation

- Set the thermal conductivity to 0.25, which agrees with all of the data at temperatures below 800 K, and agrees somewhat with the correlation of Atkinson and Merrick at even higher temperatures.

16

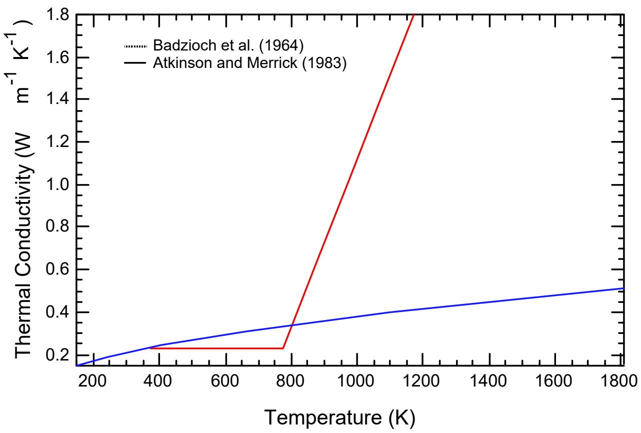


Comparison of thermal conductivity correlations from Atkinson and Merrick (1983) and Badzioch et al. (1964).

17

# Single Particle Energy Equation

- Temperature form

$$m_p C_p \frac{dT_p}{dt} = \theta h A_p \left(T_g - T_p\right) + \varepsilon \sigma A_p \left(T_w^4 - T_p^4\right) + \sum_i r_{pi} \, \Delta H_{rxn,i}$$

- Enthalpy form

$$\frac{d\left(m_p h_p\right)}{dt} = Q_{rp} + Q_{cp} - r_p h_{pg}$$

- where

$$h_{pg} = \frac{\sum r_{vol,i} h_{vol,i} + h_{char} \sum r_{char,i}}{r_{tot}}$$

18

## Particle Size Distribution

- In general, means are defined as:

$$x_m = \frac{\int_a^b x\,df}{\int_a^b df} = \frac{\sum_{i=1}^{n} x_i f_i}{\sum_{i=1}^{n} f_i}$$

- Mass mean:

$$d_m = \sum_{i=1}^{n} d_i w_i, \quad where \quad \sum_{i=1}^{n} w_i = 1$$



## Particle Size Distributions (cont.)

- Mass per particle: $m_p = \rho \frac{4}{3} \pi r^3$

- Number of particles = mass/(mass per particle)
- Number mean becomes:

$$d_n = \frac{\sum_{i=1}^{n} d_i \left( \frac{6w_i}{\rho\pi d_i^3} \right)}{\sum_{i=1}^{n} \left( \frac{6w_i}{\rho\pi d_i^3} \right)_i} = \frac{\sum_{i=1}^{n} d_i \left( \frac{w_i}{d_i^3} \right)}{\sum_{i=1}^{n} \left( \frac{w_i}{d_i^3} \right)_i}$$

Please compute the number distribution (# vs. diameter in microns) for the following mass distribution

| Mesh Size (passing) | 400 | 325 | 270 | 250 | 200 | 170 | 140 |
|---|---|---|---|---|---|---|---|
| Weight (%) | 5 | 10 | 20 | 30 | 20 | 10 | 5 |

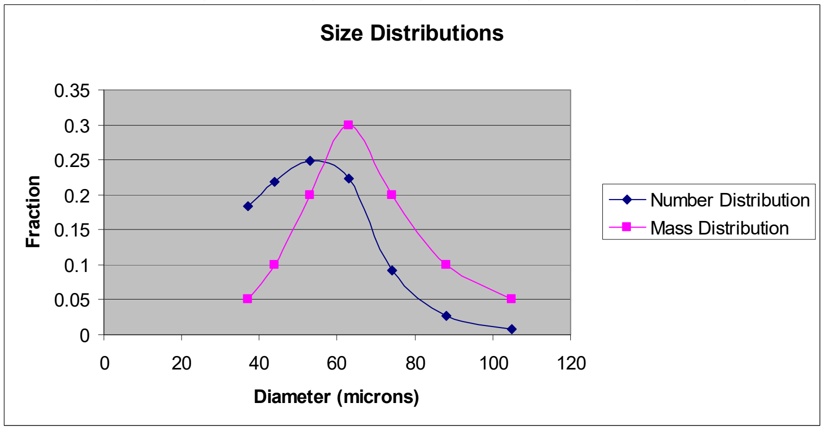


**Number mean = 53.6 $\mu$m**
**Mass mean = 64.6 $\mu$m**

21

**Table 21-12. U.S. Sieve Series and Tyler Equivalents**
(A.S.T.M.—E-11-61)

| Sieve designation: Standard | Sieve designation: Alternate | Sieve opening: mm. | Sieve opening: in. (approx. equivalents) | Nominal wire diam.: mm. | Nominal wire diam.: in. (approx. equivalents) | Tyler equivalent designation |
|---|---|---|---|---|---|---|
| 107.6 mm. | 4.24 in. | 107.6 | 4.24 | 6.40 | 0.2520 | |
| 101.6 mm. | 4 in.† | 101.6 | 4.00 | 6.30 | .2480 | |
| 90.5 mm. | 3½ in. | 90.5 | 3.50 | 6.08 | .2394 | |
| 76.1 mm. | 3 in. | 76.1 | 3.00 | 5.80 | .2283 | |
| 64.0 mm. | 2½ in. | 64.0 | 2.50 | 5.50 | .2165 | |
| 53.8 mm. | 2.12 in. | 53.8 | 2.12 | 5.15 | .2028 | |
| 50.8 mm. | 2 in.† | 50.8 | 2.00 | 5.05 | .1988 | |
| 45.3 mm. | 1¾ in. | 45.3 | 1.75 | 4.85 | .1909 | |
| 38.1 mm. | 1½ in. | 38.1 | 1.50 | 4.59 | .1807 | |
| 32.0 mm. | 1¼ in. | 32.0 | 1.25 | 4.23 | .1665 | |
| 26.9 mm. | 1.06 in. | 26.9 | 1.06 | 3.90 | .1535 | 1.050 in. |
| 25.4 mm. | 1 in.† | 25.4 | 1.00 | 3.80 | .1496 | |
| 22.6 mm.* | ⅞ in. | 22.6 | 0.875 | 3.50 | .1378 | 0.883 in. |
| 19.0 mm. | ¾ in. | 19.0 | .750 | 3.30 | .1299 | .742 in. |
| 16.0 mm.* | ⅝ in. | 16.0 | .625 | 3.00 | .1181 | .624 in. |
| 13.5 mm. | 0.530 in. | 13.5 | .530 | 2.75 | .1083 | .525 in. |
| 12.7 mm. | ½ in.† | 12.7 | .500 | 2.67 | .1051 | |
| 11.2 mm.* | 7/16 in. | 11.2 | .438 | 2.45 | .0965 | .441 in. |
| 9.51 mm. | ⅜ in. | 9.51 | .375 | 2.27 | .0894 | .371 in. |
| 8.00 mm.* | 5/16 in. | 8.00 | .312 | 2.07 | .0815 | 2½ mesh |
| 6.73 mm. | 0.265 in. | 6.73 | .265 | 1.87 | .0736 | 3 mesh |
| 6.35 mm. | ¼ in.† | 6.35 | .250 | 1.82 | .0717 | |
| 5.66 mm.* | No. 3½ | 5.66 | .223 | 1.68 | .0661 | 3½ mesh |
| 4.76 mm. | No. 4 | 4.76 | .187 | 1.54 | .0606 | 4 mesh |
| 4.00 mm.* | No. 5 | 4.00 | .157 | 1.37 | .0539 | 5 mesh |
| 3.36 mm. | No. 6 | 3.36 | .132 | 1.23 | .0484 | 6 mesh |
| 2.83 mm.* | No. 7 | 2.83 | .111 | 1.10 | .0430 | 7 mesh |
| 2.38 mm. | No. 8 | 2.38 | .0937 | 1.00 | .0394 | 8 mesh |
| 2.00 mm.* | No. 10 | 2.00 | .0787 | 0.900 | .0354 | 9 mesh |
| 1.68 mm. | No. 12 | 1.68 | .0661 | .810 | .0319 | 10 mesh |
| 1.41 mm.* | No. 14 | 1.41 | .0555 | .725 | .0285 | 12 mesh |
| 1.19 mm. | No. 16 | 1.19 | .0469 | .650 | .0256 | 14 mesh |
| 1.00 mm.* | No. 18 | 1.00 | .0394 | .580 | .0228 | 16 mesh |
| 841 micron | No. 20 | 0.841 | .0331 | .510 | .0201 | 20 mesh |
| 707 micron* | No. 25 | .707 | .0278 | .450 | .0177 | 24 mesh |
| 595 micron | No. 30 | .595 | .0234 | .390 | .0154 | 28 mesh |
| 500 micron* | No. 35 | .500 | .0197 | .340 | .0134 | 32 mesh |
| 420 micron | No. 40 | .420 | .0165 | .290 | .0114 | 35 mesh |
| 354 micron* | No. 45 | .354 | .0139 | .247 | .0097 | 42 mesh |
| 297 micron | No. 50 | .297 | .0117 | .215 | .0085 | 48 mesh |
| 250 micron* | No. 60 | .250 | .0098 | .180 | .0071 | 60 mesh |
| 210 micron | No. 70 | .210 | .0083 | .152 | .0060 | 65 mesh |
| 177 micron* | No. 80 | .177 | .0070 | .131 | .0052 | 80 mesh |
| 149 micron | No. 100 | .149 | .0059 | .110 | .0043 | 100 mesh |
| 125 micron* | No. 120 | .125 | .0049 | .091 | .0036 | 115 mesh |
| 105 micron | No. 140 | .105 | .0041 | .076 | .0030 | 150 mesh |
| 88 micron* | No. 170 | .088 | .0035 | .064 | .0025 | 170 mesh |
| 74 micron | No. 200 | .074 | .0029 | .053 | .0021 | 200 mesh |
| 63 micron* | No. 230 | .063 | .0025 | .044 | .0017 | 250 mesh |
| 53 micron | No. 270 | .053 | .0021 | .037 | .0015 | 270 mesh |
| 44 micron* | No. 325 | .044 | .0017 | .030 | .0012 | 325 mesh |
| 37 micron | No. 400 | .037 | .0015 | .025 | .0010 | 400 mesh |

From Perry's Chemical Engineers' Handbook

22

follow some distribution, such as the **Rosin-Rammler-Bennett** [Rosin and Rammler, *J. Inst. Fuel*, 7, 29–36 (1933); Bennett, *ibid.*, **10**, 22–39 (1936)]:

$$Y = 1 - \left[\exp - \left(\frac{X}{X'}\right)^n\right] \qquad (8\text{-}1)$$

or the **Gates-Gaudin-Schumann** distribution [Schumann, *A.I.M.E. Tech. Paper* 1189, *Mining Tech.* (1940)]:

$$Y = \left(\frac{X}{k}\right)^m \qquad (8\text{-}2)$$

or the **logarithmic-probability** distribution [Hatch and Choate, *J. Franklin Inst.*, **207**, 369 (1929)]:

$$Y = \text{erf}\left(\frac{\ln X/X'}{\sigma}\right) \qquad (8\text{-}3)$$

or the **Gaudin-Meloy** distribution [Gaudin and Meloy, *Trans. A.I.M.E.*, **223**, 40–50 (1962)]:

$$Y = 1 - \left(1 - \frac{X}{X'}\right)^r \qquad (8\text{-}4)$$

where $Y$ = cumulative fraction by weight undersize; $X$ = size; $k$, $X'$ = parameters with dimension of size; $m$, $n$, $r$ = dimensionless

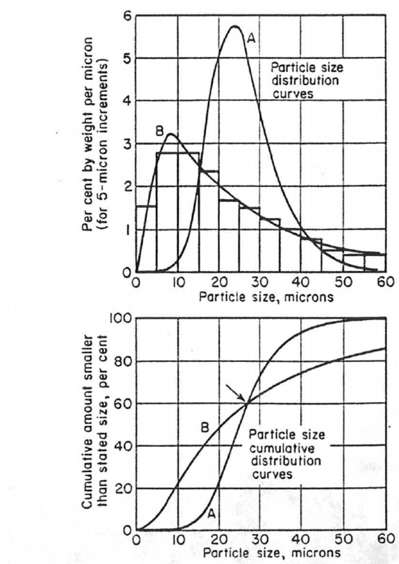


Fig. 8-1. Particle-size distribution curves for simple powders.

From Perry's Chemical Engineers' Handbook

23

# Rosin-Rammler Distribution

(similar to a Weibull distribution)

$$f = 1 - e^{-\left(\frac{d}{a}\right)^n}$$

where *f* is the cumulative weight fraction under size *d*, and *a* and *n* are fitting parameters.

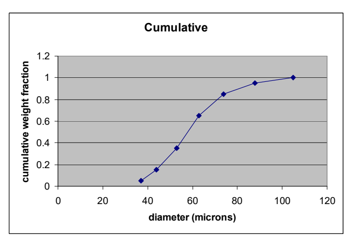


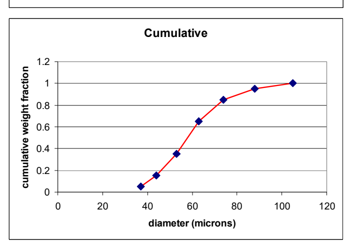


24

# Internal Surface Areas

- Internal surface areas are measured by adsorption of some gas ($N_2$, $CO_2$, $O_2$, Ar)
- Units are generally $m^2/g$
- Raw coal generally has less surface area than char (after devolatilization)
- $CO_2$ method generally gives larger internal surface area than $N_2$ method
- No method is accepted as standard

25

# Internal Surface Area Data

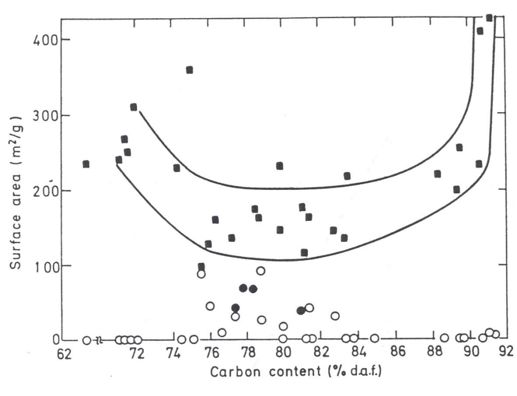


*Figure 1* Variation of nitrogen and carbon dioxide surface areas of coals with carbon content
● $N_2$ (from reference 14), ○ $N_2$ (determined), ■ $CO_2$

From Gan et al. Fuel, Vol. 51 (1972)

26

# $N_2$ Internal Surface Area Data

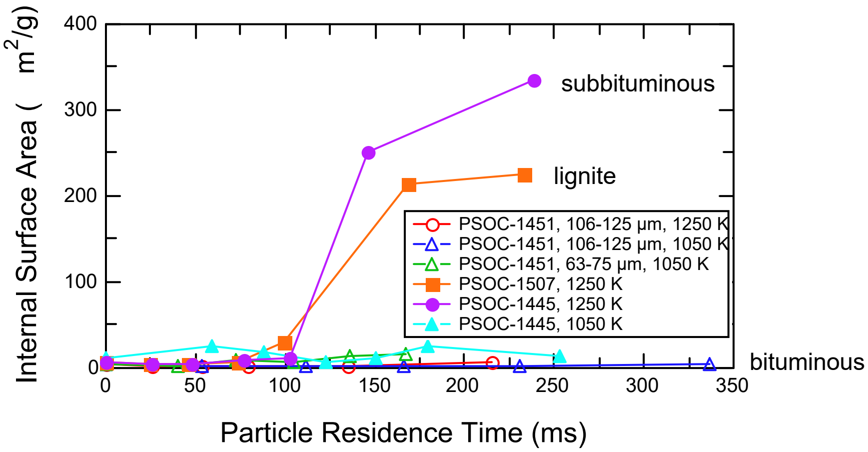


Internal surface areas of char particles from different coals as a function of residence time, as measured by the $N_2$ BET method.
From Fletcher Sandia Milestone Report

27

# Heating Value

- A common terminology has been adopted in the United States regarding the heating value of coal. The term "high heating value" is defined to be the calorific value of coal, computed as if the water ($H_2O$) products of coal combustion end up in the liquid form.
- In other words,
- C ==> $CO_2$ (gas)
- H ==> $H_2O$ (liquid)
- O ==> $O_2$ (gas), which helps burn the C, H, and S
- N ==> $N_2$ (gas)
- S ==> $SO_2$ (gas)

- $Q_h$ = 145.44 (%C) + 620 [(%H) - (%O)/8] + 41(%S) (Btu/lb) (DuLong formula)
- $Q_l = Q_h$ - 92.7 (%H) (Btu/lb)

(daf compositions)

($Q_l$ and $Q_h$ are positive when exothermic)

(from Perry's Chem. Eng. Handbook)

28

# Heating Value (cont.)

**Note:**

- **If the high heating value of the coal is defined to have the hydrogen products end up as $H_2O$ (liq.), then the latent heat of moisture evaporation is automatically removed from the problem.**
- **% moisture = %H2O (liq.) ==> H2O (liq.) $\Delta H_{react}$ = 0.0**
- **So:**

$$\frac{Q_h\left(Btu/lb\ of\ \ wet,\ ash-included\ \ coal\right)}{\left(1-x_{ash}-x_{moist}\right)}=Q_h\left(Btu/lb\ of\ \ daf\ \ coal\right)$$

29

# Other Heating Value Correlations

$$Q_s = 338.3\mathrm{C} + 1443\left(\mathrm{H} - \frac{\mathrm{O}}{8}\right) + 94.2\mathrm{S} \qquad (1)$$

$$Q_s = 340.6\mathrm{C} + 14324\mathrm{H} - 153.2\mathrm{O} + 104.7\mathrm{S} \qquad (2)$$

$$Q_s = 339.1\left(\mathrm{C} - \frac{3}{8}\mathrm{O}\right) + 238.6\left(\frac{3}{8}\mathrm{O}\right) + 1444\left(\mathrm{H} - \frac{1}{16}\mathrm{O}\right) + 104.7\mathrm{S} \qquad (3)$$

$$Q_s = 339.1\mathrm{C} + 1433.7\mathrm{H} + 93.1\mathrm{S} - 127.3\mathrm{O} \qquad (4)$$

$$Q_s = 519\mathrm{C} + 1625\mathrm{H} + \mathrm{O}^2 - 17870 \qquad (5)$$

$$Q_s = 340.3\mathrm{C} + 1243.2\mathrm{H} + 62.8\mathrm{N} + 190.9\mathrm{S} - 98.4\mathrm{O} \qquad (6)$$

$$Q_s = 351.7\mathrm{C} + 1162.6\mathrm{H} + 104.7\mathrm{S} - 111\mathrm{O} \qquad (7)$$

$$Q_s = 341.4\mathrm{C} + 1444.5\mathrm{H} - \frac{1000(\mathrm{N} + \mathrm{O} - 1)}{8} + 93\mathrm{S} \qquad (8)$$

$$Q_s = 341\mathrm{C} + 1323\mathrm{H} + 68.5 - 119.4(\mathrm{O} + \mathrm{N}) \qquad (9)$$

$$Q_s = 349.1\mathrm{C} + 1178{,}3\mathrm{H} + 100.5\mathrm{S} - 103.4\mathrm{O} - 15\mathrm{N} \qquad (10)$$

$$Q_s = 339\mathrm{C} + 1214\left(\mathrm{H} - \frac{\mathrm{O}}{8}\right) + 104\mathrm{S} + 226\mathrm{H} \qquad (11)$$

30

[7] Channiwala SA, Parikh PP. A unified correlation for estimating HHV of solid, liquid and gaseous fuels. Fuel 2002;81:1051-63.
[8] Selvig WA, Gibson FH. Calorific value of coal. In: Lowry HH, editor. Chemistry of coal utilization , vol. 1, New York: Wiley; 1945, p. 139.
[9] Strache H, Lant R. Kohlenchemie. Leipzig: Akademische Verlagsgesellschaft; 1924.
[10] Steuer W.: Brennstoff-Chem, vol. 7, 1926, p. 344 according: Channiwala S.A., Parikh P.P.: A unified correlation for estimating HHV of solid, liquid and gaseous fuels. Fuel 2002;81:1051.
[11] D'Huart K.: Die Warme, vol. 53, 1930, p. 313 Chem Abstr., vol. 24, 1930, p. 5966 according: Channiwala S.A., Parikh P.P.: A unified correlation for estimating HHV of solid, liquid and gaseous fuels. Fuel 2002;81:1051.
[12] Seylor A.C.: Proc S Wales Inst Engrs., vol. 53, 1938, p. 254 according: Channiwala S.A., Parikh P.P.: A unified correlation for estimating HHV of solid, liquid and gaseous fuels. Fuel 2002;81:1051.
[13] Gumz W.: Feuerungstech, vol. 26, 1938, p. 322. Chem Abstr., vol. 33, 1939, p. 6556 according: Channiwala S.A., Parikh P.P.: A unified correlation for estimating HHV of solid, liquid and gaseous fuels. Fuel 2002;81:1051.
[14] Boie W.: Energietechnik, vol. 3, 1953, p. 309 according: Channiwala S.A., Parikh P.P.: A unified correlation for estimating HHV of solid, liquid and gaseous fuels. Fuel 2002;81:1051.
[15] Grabosky M, Bain R. Properties of biomass relevant to gasification. In: Reed TB, editor. Biomass gasification – principles and technology, New Jersey: Noyes Data Corporation; 1981, p. 41.
[16] IGT. Coal Coversion Systems Technical Data Book, DOE Contract EX 76-C-01-2286. Springfield, VA: NTIS; 1978.
[17] Ocheduszko S. Termodynamika stosowana (in Polish). WNT Warszawa; 1967.

(from Sciazko, M., 2012)

31

# Andrew Richards Paper

- DuLong and other formulas were obtained from a limited number of coals
- Re-fit data from large number of coals using proposed model forms

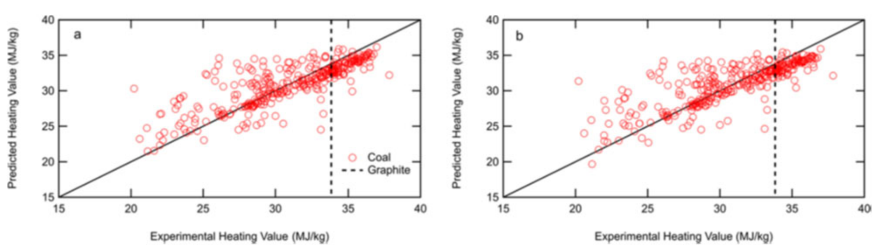


Parity plots of all best model forms for coal heating value: a) Mott-Spooner re-fit and b) Boie re-fit. Both plots include a vertical dashed line indicating the heating value of pure graphite.

Richards, A., D. Haycock, J. Frandsen, and T. H. Fletcher, "A Review of Coal Heating Value Correlations with Application to Coal Char, Tar, and Other Fuels," *Fuel*, 118942:1-16 (2021). **DOI:** 10.1016/j.fuel.2020.118942

32